ELSEVIER

Biochimica et Biophysica Acta 1597 (2002) 12–21

BIOCHIMICA ET BIOPHYSICA ACTA
BBA

www.bba-direct.com

Temperature-induced β-aggregation of fibronectin in aqueous solution

E. Pauthe [a], J. Pelta [a,*], S. Patel [a], D. Lairez [b], F. Goubard [c]

[a] *ERRMECE, Université de Cergy-Pontoise, 2 Avenue Adolphe Chauvin, 95302 Cergy-Pontoise cedex, France*
[b] *Laboratoire Léon Brillouin, CEA-CNRS, CEA/Saclay, 91191 Gif-sur-Yvette cedex, France*
[c] *LCMI, Université de Cergy-Pontoise, 95031 Cergy-Pontoise cedex, France*

Received 10 October 2001; received in revised form 25 January 2002; accepted 25 January 2002

Abstract

Fibronectin structural reorganization induced by temperature has been investigated by Fourier-transform infrared (FT-IR) spectroscopy and light-scattering experiments. At 20 °C, from resolution enhanced by FT-IR spectra, 43% of β sheet, 31% of turn and 26% of unordered structures were estimated. Static and quasi-elastic light-scattering results do not change significantly between 20 and 34 °C. Just below 50 °C, a decrease of 1/3 of β sheet structures contents is observed, concomitantly with a corresponding increase of turn. The contribution of disordered structures is found to be temperature-independent. Above 50 °C, our data reveals the formation of intermolecular hydrogen bonding leading to the formation of intermolecular β sheet structures. The IR band absorption at 1618 cm^{-1} increases strongly as a function of temperature. The scattered intensity increases and becomes strongly q^2-dependent. The dynamic structure factor is not a single exponential decay and becomes strongly dependent on the scattering angle. These results demonstrate that aggregation occurs in fibronectin solution. When temperature decreases, this aggregation is found irreversible. Fibronectin aggregation is driven by the formation of intermolecular hydrogen bonds responsible for intermolecular β sheet structures.

Keywords: Fourier-transform infrared; β-Aggregation; Fibronectin

1. Introduction

Fibronectin is a large glycoprotein (molecular mass = 530 kg/mol), composed of two nearly identical covalently linked subunits. This protein, circulating in the blood and in the plasma, could be transformed by cultured fibroblasts into an insoluble fibrillar component of the extracellular matrix [1,2]. Fibronectin consists of the repetition of 56 globular modules of three types, I, II, III having a well-defined structure and high degree of internal homology. They are connected by short polypeptide segments sensitive to proteinases and are regrouped in functional domains that express specific binding activities [3]. This protein is produced by different cell types (hepatocytes, fibroblasts, macrophages, leucocytes etc...). Fibronectin mediates cell adhesion and migration in a wide variety of biological processes. It probably plays a significant role in wound healing, embryogenesis, phagocytosis, cell transformation, locomotion and hemostasis [1,4].

Under plasmatic buffer conditions, at room temperature, the conformation of fibronectin has been investigated by several techniques. It has been shown that fibronectin conformation implies both large-scale flexibility and local order [5–12]. Recently, light-scattering and small angle neutron-scattering results have shown that the native fibronectin conformation is consistent with a Gaussian chain of 56 globular modules [13].

X-ray crystallography and NMR spectroscopy have been successfully used to elucidate the structure of some individual modules or short fragments [14–19]. Their structure was found as being mainly β sheet. However, these techniques cannot be used in the study of the secondary structure of the whole fibronectin because its random conformation prevents crystallization [13]. Consequently, for this protein, the structure determination by Fourier-transform infrared spectroscopy (FT-IR) becomes very useful because it can be achieved in solution.

The structure of absorbed fibronectin on surfaces with different compositions was studied by Cheng et al. [20] using FT-IR and total internal reflection. The data show that the ratio of the β sheet to the β turn structures increases with adsorption time and changes with surfaces. This study demonstrated that different chemical end groups on the

Abbreviation: FSD, Fourier self deconvolution

* Corresponding author. Tel.: +33-1-3425-6604; fax: +33-1-3425-6552.
E-mail addresses: pelta@u-cergy.fr, Juan.pelta@bio.u-cergy.fr (J. Pelta).

0167-4838/02/$ - see front matter
PII: S0167-4838(02)00271-6

substratum modulate fibronectin conformation but have no effect on the amount of proteins bound.

The fibronectin structure modification upon heating, has been mainly studied on fibronectin fragments. Litvinovich et al. [21,22] have studied by scanning calorimetry and fluorescence spectroscopy, the melting behavior of the 110-kDa cell-binding fragment (III_2–III_{11} module) and of the ninth type III module. The main results show that the 110-kDa fragment, central region of fibronectin, includes 10 independently folded type III domains, almost of which, interacts with each other. These domains exhibit a wide range of thermal stability. The partially unfolded type III_9 module undergoes rapid self-association leading to the formation of large stable multimers that retain substantial amounts of β sheet structure. Such structural organizations possibly playing a role in the regulation of matrix assembly or interactions with other molecules such as integrin receptors on cell surfaces. Recent molecular dynamics simulations data, from Paci and Karplus [23], shows the temperature-induced unfolding of fibronectin type III module. The main results are a partial separation of the β sandwich and the unfolding of the individual sheets in a stepwise fashion.

As for the whole fibronectin, few studies are concerned by its structure and conformation upon heating. They are based on the local scale investigation using circular dichroism or fluorescence spectroscopy [7,8], or on a larger-scale investigation of hydrodynamic properties [10]. The main results of these studies are: (i) very little unfolding occurs below a temperature of the order of 50 °C, (ii) above this temperature, up to 75 °C, an incomplete exposure of tryptophanyl groups to water is found, (iii) values of the diffusion coefficient do not change significantly between 10 and 37 °C.

No systematic study concerned with the temperature-induced structural and conformation changes of the whole fibronectin, has been reported. In this paper, we report a study of fibronectin local structure and conformation upon heating, by FT-IR spectroscopy and light-scattering. Our data show that fibronectin aggregation is driven by the formation of intermolecular hydrogen-bonding, leading to the formation of intermolecular β sheets. When the temperature is decreased, this process is found irreversible. Temperature structural changes on fibronectin are discussed in terms of denaturation, aggregation and gelation. Possible biological implications of β aggregation are also discussed in term of fibril formation.

2. Materials and methods

2.1. Fibronectin preparation

Fibronectin was purified from cryoprecipitated human plasma according to a three-step protocol recently developed in our laboratory. This protocol is based on fibronectin affinities for both gelatin and heparin as previously described [24]. It yields high quantity and purity protein (98.6 ± 1.2%) as monitored by densitometry analysis of silver nitrate stained SDS-PAGE (polyacrylamide gel elec-

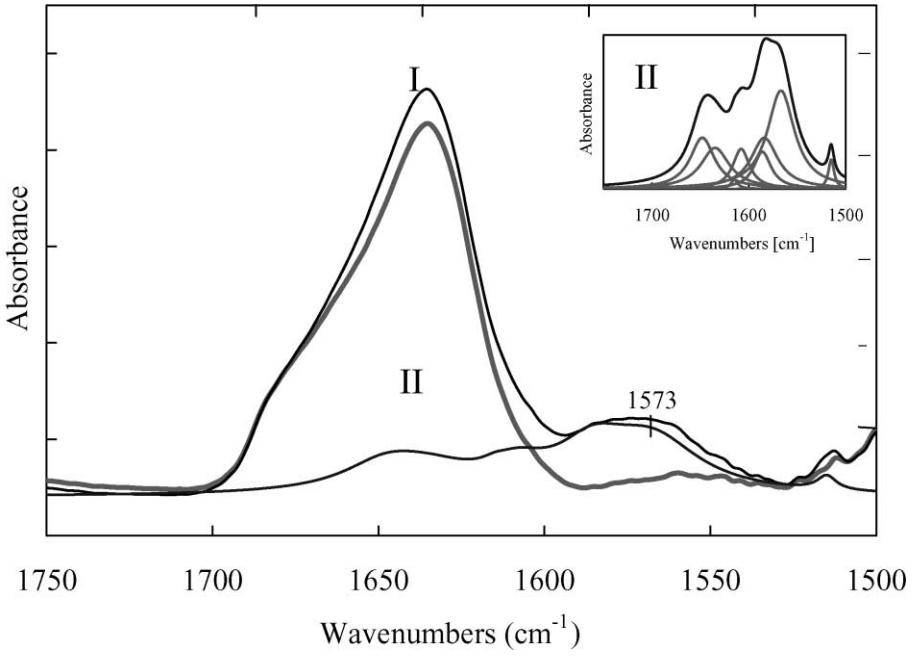

Fig. 1. FT-IR spectra of deuterated fibronectin and amino acid side chain group contribution in the amide I′ region. Original protein spectra (I), amino acid side chain group absorption of fibronectin (II), as calculated from a set of individual amino acid side chain group spectra according to the amino acid composition of fibronectin (see inset). Spectra drawn in grey represent the difference between (I) and (II), i.e. the "original" FT-IR fibronectin spectra in the amide I′ region without the fibronectin's amino acid contribution.

trophoresis). All experiments were performed in a 10 mM Tris–HCl (pH 7.4) buffer containing 150 mM NaCl, which corresponds to plasmatic conditions. Fibronectin solution was concentrated, using Ultrafree-15 centrifugal concentrators from Millipore (100 kDa cutoff). Protein concentration was determined using the absorbance at 280 nm, knowing that an absorbance of 1.28 corresponds to a concentration of 1 mg/ml [25].

2.2. Fluorescence spectroscopy

Fluorescence spectroscopic measurements were carried out on a Perkin-Elmer LS-50B luminescence spectrometer equipped with a constant temperature cell holder. A 3 ml standard quartz cell of 1 cm path length was used. For tryptophan fluorescence of the protein, excitation wavelength is 295 nm, emission spectra are recorded between 310 and 400 nm, with 10 and 5 nm slit widths for excitation and emission, respectively. Protein concentration was 0.1 μM in H_2O or D_2O in the buffer described above (10 mM Tris–HCl, 150 mM NaCl).

2.3. Fourier-transformed infrared spectroscopic measurement

FT-IR spectroscopy is known to be efficient on the study of the secondary structure of the protein backbone [26–29]. The 1600–1700 cm^{-1} region of FT-IR protein spectra (amide I′ band) is mainly due to the C=O stretching vibration but also partly due to C–N stretching vibration of polypeptide bonds. This region is thus very sensitive to the secondary structure of proteins.

IR spectra were collected using a Bruker IFS-55 FT-IR spectrometer equipped with a DGTS detector. The protein solutions were placed in homemade demountable cells with CaF_2 windows and a 6 μm path length spacer. The samples were thermostated using a cell jacket of circulating water and the temperature was measured with a thermocouple placed near the cell window. FT-IR spectra of the protein solutions and of the control buffers were recorded using identical scanning parameters. Typically for each spectrum, 256 interferograms were accumulated and co-added in a single-beam mode at a resolution of 2 cm^{-1} and Fourier-transformed infrared using Happ/Genzel apodization function. To eliminate the spectral contributions of atmospheric water vapor, the instrument was continuously purged with dry air. Buffer spectra was subtracted using the 1209 cm^{-1} band due to D_2O as a reference, thereby avoiding artificial bands and/or incorrect band positions in the amide I′ region of the protein spectrum.

For these measurements, fibronectin solution at a concentration of 20 mg/ml is dialyzed during 12 h using a microdialysis cassette (Slide-A-Lyser, 10 000 MW cutoff, Pierce, Rockford, IL) against a 100-fold volume of D_2O buffer at plasmatic pH and ionic strength. Dialysis is performed at temperatures ranging from 20 to 25 °C. Reagent grade deuterated water (D_2O) was purchased form (Eurisotop, Saclay, France).

To compare the amide I′ absorption area at different temperatures, a baseline was subtracted in order to ensure a zero absorbance in the featureless region of the spectrum between 1590 and 1710 cm^{-1}. After baseline subtraction, the band was treated using FSD, the second and the fourth-derivative methods. This treatment allows the evaluation of the number of peaks and their positions in the amide I′ band. The deconvolution of the infrared spectra was done as described by Kauppinen et al. [30]. The best deconvolution factors have been fixed: the half-bandwidth was 15 cm^{-1} with band-narrowing factor of 2.4. Areas of these peaks were estimated by using standard curve-fitting procedures [31]. Initial values for peak heights and widths were estimated visually from the deconvoluted spectra. A Gaussian profile was used as a parameter for the envelope of the deconvoluted spectra. For the final fits, the heights, widths and positions of all peaks were varied simultaneously.

For the study of temperature effects, protein solutions (concentration of 20 mg ml^{-1}) were heated from 20 to 80 °C.

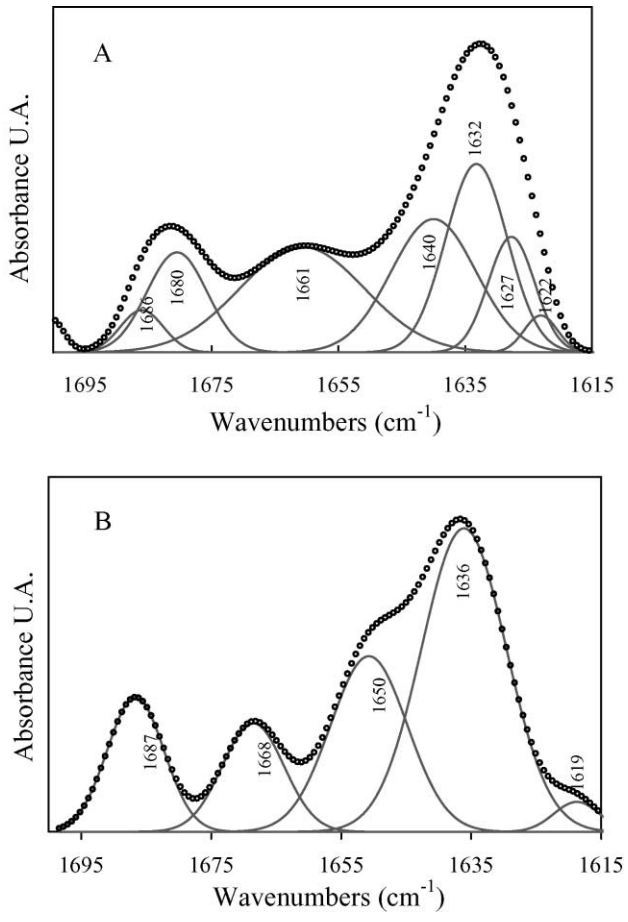

Fig. 2. Curve fitted Fourier self-deconvoluted amide I′ band of fibronectin in D_2O (A) and in H_2O (B). Fourier self-deconvolution was performed using an initial Lorentzian line-shape, $\Sigma = 15$ cm^{-1} and a resolution enhancement factor, $K = 2.4$. Curve fitted bands as individual Gaussian components are in grey; their sums are represented as filled circles.

Table 1
Secondary structure assignment of fibronectin in H_2O and D_2O buffer

(A) Curve-fitted peak positions, relative integrated intensities and secondary structures assignments of the amide I (I′) band components of fibronectin in H_2O buffer and after complete H/D exchange in D_2O buffer

H_2O			D_2O		
Band position (cm^{-1})	Band area (%)	Assignment	Band position (cm^{-1})	Band area (%)	Assignment
1687	13.8	turn	1686	3.8	β/turn
1668	12.2	turn	1680	12.9	β/turn
			1661	22.5	turn
1650	24.8	unordered	1640	25.6	unordered
1636	46.8	β strand	1632	23.1	β strand
			1627	9.8	β strand
1619	2.4	turn	1622	2.3	β strand

(B) Comparison of fibronectin secondary structure distribution by FT-IR between H_2O and D_2O buffer solution

	H_2O (%)	D_2O (%)
β sheet	47	43
Helix	–	–
Turn	28	31
Unordered	25	26

IR spectra were recorded at various intervals after temperature stabilization. To study the reversibility of temperature effects, spectra were also recorded for decreasing temperatures from 80 to 25 °C.

2.4. Scattering experiments

Details of the light-scattering experimental setup and data reduction procedure were described elsewhere [13]. Experiments were performed using Argon gas laser of wavelength $\lambda_0 = 488$ nm. The scattering vector is with θ the scattering angle and n the refractive index of the sample. Scattered intensity is measured at different scattering angle ranging from 20° to 150°. Quasi-elastic light-scattering measurements were performed computing the time-dependent autocorrelation function of the scattered intensity with a Malvern 7032 correlator. Once normalized, the autocorrelation function leads to the dynamical structure factor: $S(q,t) = \exp(-Dq^2t)$, where t is the time and D is an apparent diffusion coefficient which can be q- and

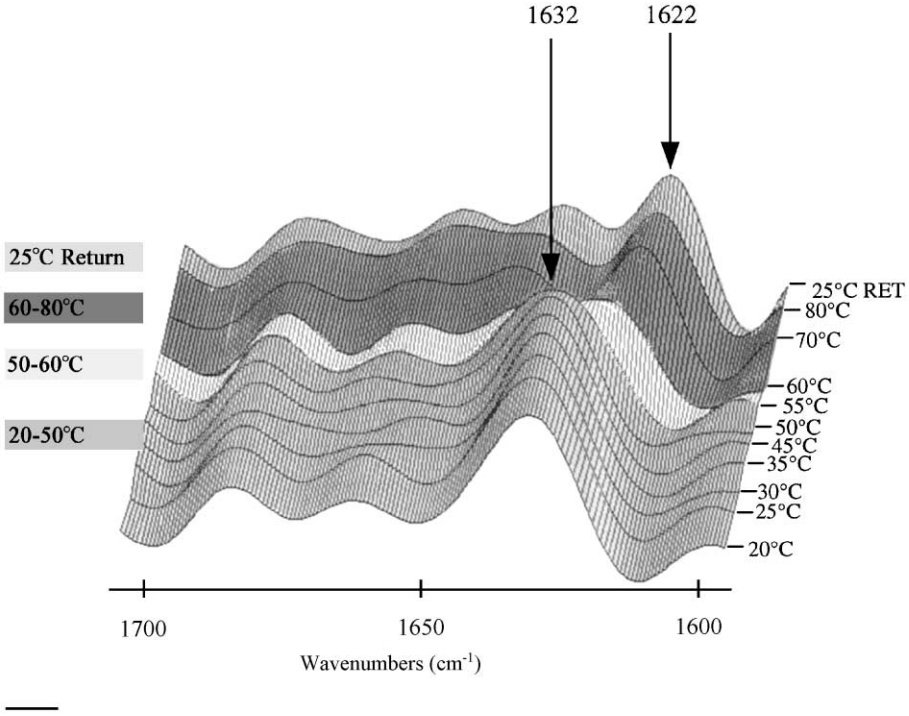

Fig. 3. Fourier self-deconvoluted FT-IR spectra of fibronectin in the amide I′ region at different temperatures. The z-axis corresponds to discrete temperature.

t-dependent. In the case of monodisperse population of small macromolecules of size R_g observed at $qR_g < 1$, and neglecting their interactions in diluted solutions, D is constant and represents the actual diffusion coefficient of the macromolecules. The hydrodynamic radius R_H is thus deduced from the Stokes–Einstein relation: $R_H=(kT)/(6\pi\eta D)$, where k is the Boltzmann constant, T is the temperature and η the solvent viscosity. Thus, in this case one has: $S(q,t) = \exp\left(-\frac{kT}{6\pi R_H} \times \frac{tq^2}{\eta}\right)$.

In the case of a polydisperse population of macromolecule aggregates, if the larger aggregates have a size R such as $qR_g \cong 1$ or $qR_g > 1$ in the investigated q-range, the apparent diffusion coefficient D is strongly q- and t-dependent [32]. In most cases, D increases with q and decreases with t. Therefore, $S(q,t)$ is no more exponential and the dynamics are not due to a single diffusion process.

3. Results

3.1. Secondary structure and deuteration

As expected, deuteration causes a shift of the amide I band, noted I′ in D_2O, compared to spectra obtained in H_2O (data not shown). Furthermore, we show that $H \rightarrow D$ exchange reaches an equilibrium after 12 h dialysis, according to the Fourier self-deconvolution (FSD) IR spectra of fibronectin, which remains unchanged in spite of a 3 days dialysis (data not shown). Moreover, from the deuteration, a peak at 1573 cm^{-1} is revealed when the amide II (II′) band shifts in D_2O solutions (Fig. 1). This peak is assigned to the vibration of amino acid side chain group of Arg, Tyr, Glu, Gln, Asp and Asn [33].

In order to get the value with the best accuracy in the contribution of the secondary structure elements of fibronectin in the amide I′ region, we have evaluated the influence of the amino acid side chain group absorption of fibronectin in this spectral region. First, taking into account the quantity of Arg, Tyr, Glu, Gln, Asp and Asn in fibronectin [34], the theoretical spectrum of these residues in the 1600–1700 cm^{-1} region is calculated from their individual spectra (see inset Fig. 1). Second, the difference between the original protein spectrum and the amino acid spectrum is calculated and compared to the original spectrum. The result shows that this subtraction stresses on the shape of the amide I′ band. Consequently, for a better assignment of the peaks and a precise secondary structure element quantification, this difference will be considered in the following as the "original" FT-IR fibronectin spectrum in the amide I′ region. Furthermore, we have observed that the amino acid absorption contribution in the region of interest is temperature-independent, allowing the use of this subtraction procedure at each temperature.

Few information are available concerning the influence of H/D exchange on the structure of proteins. In order to check that D_2O does not modify the fibronectin structure

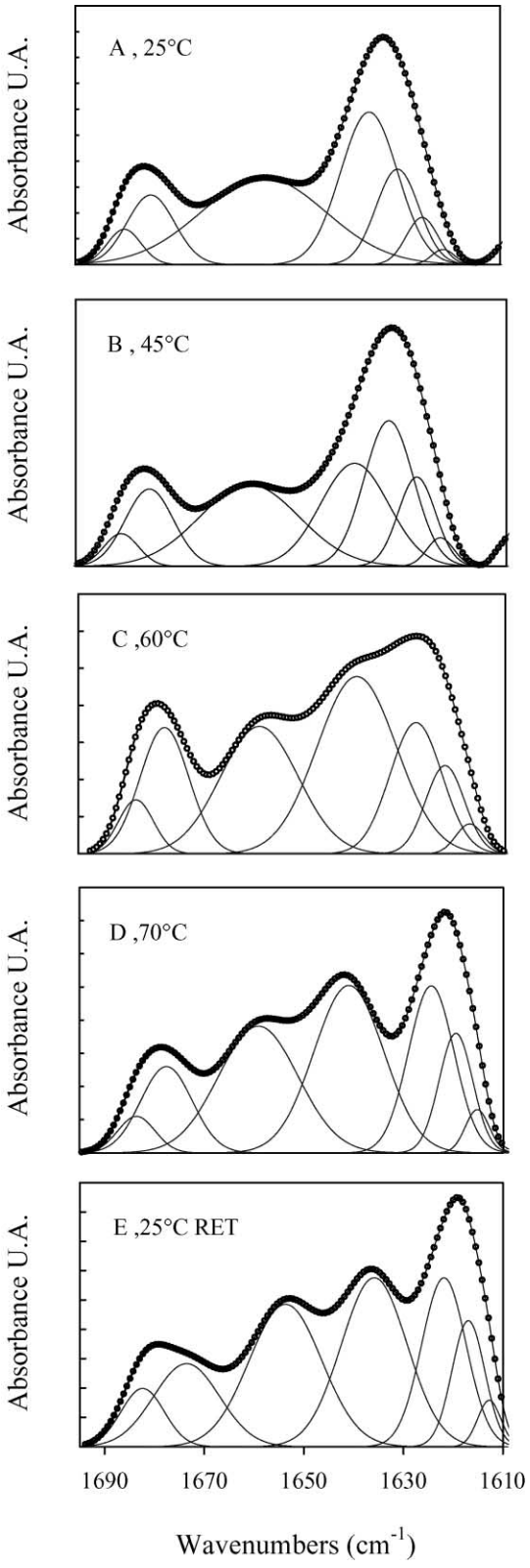

Fig. 4. Fourier self-deconvolution amide I′ band contours of fibronectin (drawn with black circles) and best fitted individual Gaussian component bands (as grey line) observed at five selected temperatures in D_2O solution.

and the effect of the temperature on this structure, (i.e., its stability), we have compared fluorescence and FT-IR spectroscopy results in H_2O and D_2O solutions.

Fluorescence spectroscopy, by measuring tryptophan emission at 360 nm, gives an indication of tryptophan exposure to water. The relative fluorescence, measured in D_2O and H_2O solutions, is plotted as a function of the temperature (see Fig. 6). For both solvents, the same fluorescence profile is obtained and the two sets of results lie on a single curve within experimental accuracy. This result shows that there is no difference in temperature effects when proteins are in D_2O and H_2O.

Fig. 2 shows the amide I′ and I band spectra resulting from the deconvolution procedure detailed in Materials and methods, in the case of D_2O (Fig. 2A) and H_2O (Fig. 2B) solutions. Relative integrated area, positions and secondary structure assignments of the different amide I or I′ band components are summarized in Table 1. Peaks are assigned from the data of Dong and Caughey [35] for H_2O and from Byler and Susi [26] for D_2O. The fibronectin is composed of 43% versus 47% of β sheets, 31% versus 28% of turns and 26% versus 25% of unordered structure in D_2O and H_2O solutions, respectively (see Table 1). Comparable secondary structure estimations are found for deuterated and non-deuterated fibronectin. This result confirms that no perceptible changes occur on native fibronectin structure due to deuteration, nevertheless, these conditions permit more precise secondary structure assignments.

3.2. Temperature effects on secondary structure

Fig. 3 shows the amide I′ band spectra of fibronectin at different increasing temperatures ranging from 20 to 80 °C and after cooling back to 25 °C.

- Between 20 and 50 °C, the shape of the spectra does not change significantly, suggesting no important changes in the fibronectin secondary structure. On the contrary, drastic changes of spectra are observed above 50 °C. Particularly, a shift of the main peak from 1632 cm^{-1} to weaker energy is observed.
- From 50 to 60 °C, intermediate spectra were observed. At 80 °C, the temperature effect is maximum with the main peak positioned at 1622 cm^{-1}. Furthermore, some changes occur in the range 1615–1620 cm^{-1}, corresponding to the appearance of a peak in this region. Moreover, the well-defined peak at 1685 cm^{-1} shifts toward the lower energy. These modifications are irreversible and very few differences are observed between spectrum measured at 80 °C and after cooling back to 25 °C. In order to have quantitative estimations of the observed changes, all these features are emphasized using curve-fitting techniques.

Typical results of curve fitting of the deconvoluted amide I′ band of fibronectin at 25, 45, 60, 70 and cooling back to 25 °C are shown in Fig. 4. Table 2 lists the peak positions and relative areas of the individual components of the spectra at the different temperatures. Several observations can be made from Table 2.

First, regarding curve-fitting spectra at 25 and 45 °C (Fig. 4A and B), the shape of the amide I′ band is not very altered, however, we observe a decrease of the relative intensity of the band components in the region of β sheet structures (at 1622, 1625, 1632 cm^{-1} and at 1680, 1686 cm^{-1} for half contribution). Conversely, we observe a corresponding increase of the band component corresponding to turn conformation (at 1661 cm^{-1} and at 1680, 1686 cm^{-1} for half contribution). No systematic change is found for the band component at 1640 cm^{-1} assigned to unordered conformation [26]. Thus, the secondary structure of fibronectin is modified progressively in the temperature range between 20 and 50 °C, with a transformation of 1/3 of the β sheets contents in turns.

Second, above 50 °C, the intensity of the band components corresponding to β sheet structures increased and

Table 2
Peak positions (cm^{-1}) and relative integrated intensities (%) of the amide I′ band components of fibronectin at different temperatures

	Temperature (°C)										
	20	25	30	35	45	50	55	60	70	RET	
Peak position	1622	1622	1622	1621	1621	1621	1621	1617	1615	1613	β
(%)	2.3	2.2	2.0	1.2	1.1	1.2	1.7	1.9	2.5	2.5	
Peak position	1626	1626	1626	1625	1626	1625	1626	1622	1620	1617	β
(%)	9.8	9.2	8.4	5.5	5.0	5.3	7.1	7.9	10.0	9.8	
Peak position	1632	1632	1632	1631	1631	1631	1631	1628	1625	1622	β
(%)	23.1	21.0	19.7	16.4	13.7	14.8	17.7	15.9	18.9	17.9	
Peak position	1640	1640	1639	1637	1636	1637	1639	1640	1641	1636	unordered
(%)	25.6	26.9	28.8	25.6	29.1	27.5	31.4	32.6	30.0	26.4	
Peak position	1661	1661	1661	1657	1657	1657	1660	1659	1659	1654	turn
(%)	22.5	22.6	22.8	34.5	36.1	35.0	24.1	23.0	25.0	24.5	
Peak position	1680	1680	1680	1679	1680	1680	1679	1678	1678	1674	β/turn
(%)	12.9	14.0	14.3	10.9	11.0	11.3	14.2	14.3	11.0	13.0	
Peak position	1686	1686	1686	1685	1685	1685	1684	1684	1684	1682	β/turn
(%)	3.8	4.1	4.0	5.9	4.0	4.9	3.6	4.2	3.4	5.9	

RET represents the sample measured at 20 °C after thermal event at 80 °C.

conversely the intensity of the component assigned to turn conformation decreased (Fig. 4C). Furthermore, the main peak corresponding to β sheet structures located at 1631–1632 cm^{-1} shifts progressively down to 1625 cm^{-1} at 70 °C (Fig. 4D). This indicates that beyond 50 °C, structural rearrangements are implicated in the formation of "new" β sheet structures. Such a modification of the β sheet band position is usually imputed to the formation of intermolecular hydrogen bonds [36].

Third, after cooling back the protein to 25 °C (Fig. 4E), the spectrum does not show significant change compared to 70 °C. This indicates that heating irreversibly modified the protein structure.

In order to determine the β sheet structures type, the IR absorbance at 1618 cm^{-1} was measured as a function of temperature for the amide I′ band (see Fig. 6). Below 50 °C, the absorbance is very small, whereas above 50 °C, up to 70 °C, it increases strongly. This result indirectly reflects the formation of intermolecular β sheets stabilized by intermolecular hydrogen bonds and will be confirmed by light-scattering measurements.

3.3. Fibronectin aggregation as viewed by light-scattering measurements

Static light-scattering measurements were performed on fibronectin solutions at 20, 34, and 49 °C. Fig. 5A shows the normalized scattered intensity ($I/I_{20°C,q\to 0}$) as a function of the square-scattering vector. Results obtained at the two lowest temperatures are superposable and are in agreement with previous results [13]. The scattered intensity at these temperatures, displays a little q dependence due to the small size of protein compared to the light-scattering q-range. Our previous measurements, performed using light and small angle neutron scattering, lead to the value $R_g = 15.3 \pm 0.2$ nm for the radius of gyration. At 49 °C, scattered intensity increases and becomes so strongly q^2-dependent that it is not possible to measure a radius of gyration (i.e., the size deduced from a Guinier approximation is too high and not compatible with the Guinier condition $qR_g < 1$).

Quasi-elastic light-scattering measurements were performed for fibronectin solutions at the same temperatures: 20, 34, and 49 °C. In Fig. 5B, the dynamical structure factor S is plotted in a log-linear scale as a function tq^2/η, in order to account for trivial viscosity effect and q dependence for diffusive processes. For the two lowest temperatures, a single straight line is obtained regardless of the scattering angle. At these temperatures $S(q,t)$ is a simple exponential decay leading to a hydrodynamic radius in agreement with the previous value already reported: $R_H = 11.5 \pm 0.1$ nm. At 49 °C, the dynamical structure factor $S(q,t)$ is no longer a single exponential decay and becomes strongly dependent on the scattering angle.

Both static and quasi-elastic light-scattering measurements show the presence of large fibronectin aggregates in the solution at 49 °C. Above 55 °C a phase separation occurs and prevents scattering measurements.

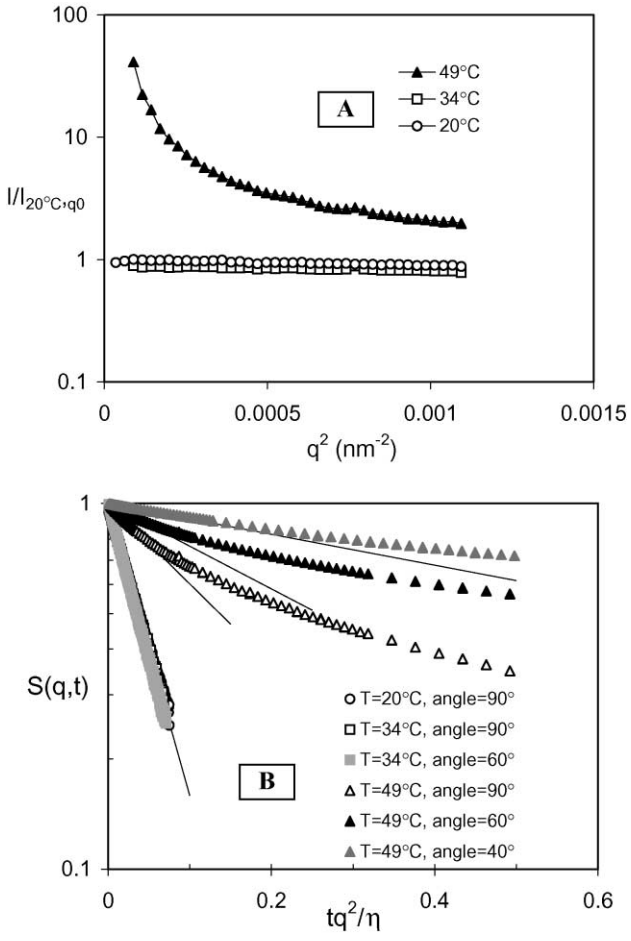

Fig. 5. Static and quasi-elastic light-scattering measurements performed at fibronectin concentration $C = 1.3$ mg/cm^3. (A) Normalized light-scattered intensity $I/I_{20\ °C,q\to 0}$ as a function of the square transfer vector q^2 for fibronectin at different temperatures. (B) Dynamical structure factor $S(q,t)$ as a function of the reduced variable tq^2/η where t is the time and η the solvent viscosity. The slope of the curves at $T = 20$ °C and $T = 34$ °C correspond to $D\eta = KT/6\pi R_H$, where D is the diffusion coefficient and R_H the hydrodynamic radius. Measurements were performed at different scattering angles. For reasons of clarity, only two angles are plotted at 34 °C. At 49 °C, the dynamical structure factor is no longer a single exponential decay.

4. Discussion and conclusion

4.1. Native fibronectin secondary structures

IR techniques in combination with second- and fourth-derivative method and Fourier self-deconvolution permit resolution enhancement of the amide I band. The accuracy of secondary structure assignment was supported by large available data [25–31,35,36]. It is thus possible to investigate the evolution of different secondary structure elements during denaturation process.

In the first part of our results, comparing the distribution secondary structure in H_2O and D_2O, it was shown that deuteration does not modify the structure and the stability of fibronectin. To our knowledge, the only previous quantitative study concerning the secondary structure of the whole fibronectin is the one of Koteliansky et al. [37] published 20 years ago. The authors report an IR study that cannot be directly compared to our results. First, because the techniques of IR data analysis have improved considerably. Second, because the authors heated their sample at 70 °C in order to ensure a complete deuteration, and here we have shown that such a heating procedure irreversibly affects the fibronectin.

Our results show that native fibronectin is composed exclusively of 43% of β sheets, 31% of turns and 26% of unordered structures. No alpha helical structure has been detected. This is in agreement with the structure of isolated modules deduced from X-ray and NMR measurements reported in the literature [14–19].

4.2. Secondary structure changes

Between 20 and 35 °C, according to FT-IR measurements, fibronectin undergoes a decrease of β sheet, 43% to 31.5%, and an increase of turns, 31% to 43%. In the same temperature range, light-scattering results do not significantly change. However, further scattering experiments at higher scattering vectors, such as small angle neutron scattering, are necessary to discuss an eventual change in the fibronectin conformation.

Temperature does not induce complete unfolding of fibronectin, whereas such an effect has been observed in urea solutions [13]. In our case, at high temperature, fibronectin aggregation occurs with a concomitant increase of intermolecular β-structure. These intermolecular bonds presumably prevent the complete protein unfolding. Temperature induces disorder, but also a concomitant decrease of the solvent quality leading to aggregation and to the formation of hydrophobic zones having a local high concentration.

We have verified that β aggregation is exclusively due to temperature effect and not of pH or mixture of both. Indeed, in our buffer condition (Tris 10 mM), a pH variation over greater than one unit over the temperature range studied could appear.

Using intrinsic fluorescence spectroscopy, we have first followed fibronectin's behavior in solution between pH 6.0 and 9.0, in order to characterize pH effect only. These results show that fibronectin structure remains unchanged in this pH range variation (data not shown).

Second, we have realized the same study as those presented in the publication at a higher ionic strength condition (Tris 100 mM), in order to minimize pH variation. These results indicate clearly that fibronectin's behavior is strictly the same (data not shown) than the one observed in our buffer condition (Fig. 6).

Cheng et al. [20] have reported studies by FT-IR with fibronectin adsorbed on surfaces leading to self-assembled monolayers. Data show an increase in the relative amount of β sheet to turn-type structure in adsorbed fibronectin as a function of time. The ratio of native to denatured protein is also expected to increase. The surface with different compositions modulates this increase. The amount of protein adsorbed to different surfaces is the same.

4.3. Protein aggregation and intermolecular β-structure

The results reported here show that fibronectin aggregation comes with the formation of intermolecular hydrogen bonds and intermolecular β-structure. The primary sequence of fibronectin contains many cysteines, accounting for a maximum of 58 disulfide bonds in the intact protein. Two intermolecular disulfide bonds join the two subunits near the COOH terminus. In each subunit, two disulfide bonds are present in every type II module and in each 12 type I modules. These numerous S–S bonds, of course, participate in the modules structuration and stabilization. However, their role is mainly local (at the module scale) so that they

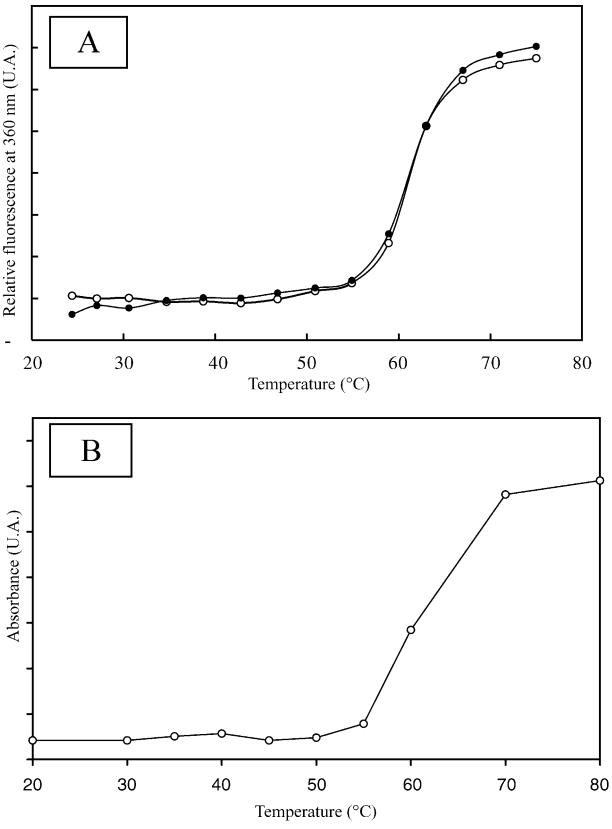

Fig. 6. (A) Fluorescence intensity emission changes of fibronectin as a function of temperature. The excitation and emission wavelength was 295 and 360 nm, respectively. Protein concentration was 0.1 μM. Emission and excitation slit was 5 and 10 nm, respectively. Fibronectin assay in H_2O buffer are drawn as white circles, assay in D_2O as black circles. (B) Temperature dependence of the peak height intensity of the amide I′ band at 1618 cm^{-1}.

trigger a limited effect on the whole fibronectin conformation. Indeed, the numerous fibronectin type III module bears no disulfide bond and the protein does not contain inter-module S–S bonds.

In the native fibronectin, from light-scattering measurement extrapolations to zero concentration of the apparent molecular mass leads to the molecular mass of 570 ± 50 kDa [13], indicating that the dimeric form is conserved. This implies the conservation of the inter-subunit S–S bonds. Furthermore, the temperature-induced effects observed here could trigger destruction and reorganization of the disulfur bonds that could in turn, contribute to irreversible aggregation. This is, however, improbable because the fibronectin modules are essentially small globular domains, which are usually stable throughout the temperature range used in this study. Example, Tm around 70–80 °C are shown for natural and recombinant type I fragments of fibronectin [38].

It is known that heat denaturation leads to a loss of secondary structures, and sometimes, to irreversible aggregation [39]. Several FT-IR studies have shown that the well-defined peaks representing the ordered structures of a native protein (as β-structures and α-helices) are replaced by (i) a band assigned to unordered structure (around 1640 cm^{-1}) or (ii) bands assigned to intermolecular bonds (around 1685 and/or 1618 cm^{-1}) [40–46]. Heat can also induce protein gelation that occurs in two steps. First, protein denaturation involves unfolding of some polypeptide segments and exposure of hydrophobic groups. Second, these hydrophobic groups tend to minimize their interfacial energy with the solvent leading to aggregation and formation of a gel network. Concomitantly, disruption of hydrogen bonds within secondary structure, β sheet as well as α-helical structures, and formation of intermolecular hydrogen bonds, were observed for instance for glycinin and β-lactoglobulin [47,48].

We have observed between 20 and 50 °C β sheet structure of the fibronectin was transformed in turns. Around physiological temperature, the global conformation of the molecule does not seem to be affected, whereas 1/3 of the β sheets change in turns.

Let us compare this result to the data reported on ribonuclease T1 by Fabian et al. [49]. This globular protein mainly includes β sheets composed of three long and two short β strands, a short two-stranded antiparallel β sheet close to the N-terminus of the protein and wide loops including several types of turns. Such secondary structures are quite similar to those of Type I and II modules of fibronectin, the authors have shown on ribonuclease T1, that near 50 °C, the β sheet decreases by 10% with a concomitant corresponding increase of turns. Their results allow to clearly identify the protein part involved in these changes, the less stable and the most exposed β sheet strands [47]. For temperatures higher than 55 °C, a simultaneous breakdown of all secondary structure components is observed during unfolding. One may suppose that similarly for fibronectin, the β sheets affected by temperature are more exposed to the solvent and less stable than those buried in the hydrophobic core region of modules.

In our study, no more structural changes are observed for temperatures higher than 55 °C, except an irreversible aggregation. The intensity of the amide I′ band component at 1618 cm^{-1} increases and reflects the intermolecular hydrogen-bonding driven by the transformation of turns in intermolecular β-structure. These intermolecular structures concern ''external'' hydrophobic regions of each module.

Litvinovich and Ingham [21] provide evidence of domain–domain interactions within the 110 kDa cell binding fragment of the fibronectin (III_2–III_{11} module). The heat capacity of this fragment is studied as a function of temperature by differential scanning calorimetry. At neutral pH, the melting of the 110 kDa fragment reveals a sharp intense peak of thermal capacity near 66 °C and a second one above 105 °C. These two exothermic peaks suggesting that the molecule contains two categories of domains: thermolabile and thermostable.

Our experimental data are compatible with Litvinovich and Ingham's study. One may suppose that these thermolabile domains are those affected at temperatures close to 55 °C for the whole protein.

4.4. Formation of fibronectin multimers and biological implication

Our results show that the partial unfolding of the fibronectin comes with self-association leading to large aggregates. Inside these aggregates, around 2/3 of the native β sheet structure are present. This result should be compared with conclusions of Litvinovich's works on the partially unfolded intermediate of the ninth type III isolated module of fibronectin. The authors have proved that this partially unfolded module undergoes rapid self-association leading to the formation of large stable multimers that, like the original monomer, contain substantial amounts of β sheet structure. The authors discussed their results in terms of a hypothetical subdomain swapping mechanism in which partially unfolded β strands regions in the module interact with complementary regions of another identical module to form oligomers and polymers. They supposed that similar phenomena might play a role in the formation of fibrils by the whole fibronectin in vivo. Such a model supposes spontaneous intermolecular linking between partially unfolded fibronectin molecules. Our results and conclusions, obtained by two complementary techniques on a highly grade-purified whole fibronectin, aims to clearly confirm these hypotheses.

Acknowledgements

We are grateful to Dr. N. Lomri for his attention to our manuscript and to M. Malika for her efficient technical assistance.

References

[1] R.O. Hynes, Fibronectins, Springer-Verlag, New York, 1990.
[2] E. Ruoslahti, Annu. Rev. Biochem. 57 (1988) 375–413.
[3] K.M. Yamada, in: D.F. Mosher (Ed.), Fibronectin, Academic Press, New York, 1989, pp. 48–121.
[4] R.O. Hynes, Proc. Natl. Acad. Sci. 96 (1999) 2588–2590.
[5] S.S. Alexander, G. Colonna, K.M. Yamada, I. Pastan, H. Edelhoch, J. Biol. Chem. 253 (1978) 5820–5824.
[6] S.S. Alexander, G. Colonna, H. Edelhoch, J. Biol. Chem. 254 (1979) 1501–1505.
[7] J.T. Edsall, G.A. Gilbert, H.A. Scheraga, J. Am. Chem. Soc. 77 (1954) 157–161.
[8] E.C. Williams, P.A. Janney, J.D. Ferry, D.F. Mosher, J. Biol. Chem. 257 (1982) 14973–14978.
[9] M. Rocco, E. Infusini, M.G. Daga, L. Gogioso, C. Cuniberti, EMBO J. 6 (1987) 2343–2349.
[10] G. Colonna, S.S. Alexander, K.M. Yamada, I. Pastan, H. Edelhoch, J. Biol. Chem. 253 (1978) 7787–7790.
[11] T.M. Price, M.L. Rudee, M. Pierschbacher, E. Ruoslahti, Eur. J. Biochem. 129 (1982) 359–363.
[12] H.P. Erickson, N. Carell, J. McDonagh, J. Cell. Biol. 91 (1981) 673–678.
[13] J. Pelta, H. Berry, G.C. Fadda, E. Pauthe, D. Lairez, Biochemistry 39 (2000) 5146–5154.
[14] C.D. Dickinson, B. Veerapandian, X.-P. Dai, R.C. Hamlin, N.-H. Xuong, E. Ruoslahti, K.R. Ely, J. Mol. Biol. 236 (1994) 1079–1092.
[15] M.J. Williams, I. Phan, T.S. Harvey, A. Rostagno, L.I. Gold, I.D. Campbell, J. Mol. Biol. 235 (1994) 1302–1311.
[16] H. Sticht, A.F. Pickford, J.R. Potts, I.D. Campbell, J. Mol. Biol. 276 (1998) 177–187.
[17] J.R. Potts, I.D. Campbell, Curr. Opin. Cell Biol. 6 (1994) 648–655.
[18] K.L. Constantine, M. Madrid, L. Banyai, M. Trexler, L. Patthy, M. Llinas, J. Mol. Biol. 223 (1992) 281–298.
[19] A.L. Main, T.S. Harvey, M. Baron, J. Boyd, I.D. Campbell, Cell 71 (1992) 671–678.
[20] S.S. Cheng, K.K. Chittur, C.N. Sukenik, L.A. Culp, K. Lewandowska, J. Colloid Interface Sci. 162 (1994) 135–143.
[21] S.V. Litvinovich, K.C. Ingham, J. Mol. Biol. 248 (1995) 611–626.
[22] S.V. Litvinovich, S.A. Brew, S. Aota, S.K. Akiyama, C. Haudenschild, K.C. Ingham, J. Mol. Biol. 280 (1998) 245–258.
[23] E. Paci, M. Karplus, J. Mol. Biol. 288 (1999) 441–459.
[24] L. Poulouin, O. Gallet, M. Rouahi, J.M. Imhoff, Protein Expression Purif. 17 (1999) 146–152.
[25] M.W. Mosesson, R.A. Umfleet, J. Biol. Chem. 21 (1970) 5728–5736.
[26] D.M. Byler, H. Susi, Biopolymers 25 (1986) 469–487.
[27] J.L.R. Arrondo, A. Muga, J. Castresana, F. Goni, Biophys. Mol. Biol. 59 (1993) 23–56.
[28] W.K. Surewicz, H.H. Mantsch, Biochim. Biophys. Acta 952 (1988) 115–130.
[29] M. Jackson, H.H. Mantsch, Crit. Rev. Biochem. Mol. Biol. 30 (1995) 95–120.
[30] J.K. Kauppinen, D.J. Moffatt, H.H. Mantsch, D.J. Cameron, Appl. Spectrosc. 35 (1981) 271–276.
[31] R.D.B. Fraser, E. Suzuki, Anal. Chem. 38 (1966) 1770–1773.
[32] E. Raspaud, D. Lairez, M. Adam, J.-P. Carton, Macromolecules 27 (1994) 2956–2964.
[33] Y.N. Chirgadze, O.V. Fedorov, N.P. Trushina, Biopolymers 14 (1975) 679–694.
[34] M. Vuento, A. Vaheri, Biochem. J. 183 (1979) 331–337.
[35] A. Dong, W.S. Caughey, Methods Enzymol. 232 (1994) 139–175.
[36] M. Jackson, H.H. Mantsch, Biochim. Biophys. Acta 1118 (1992) 139–146.
[37] V.E. Koteliansky, M.A. Glukhova, M.V. Bejanian, V.N. Smirnov, V.V. Filimonov, O.M. Zalite, S.Yu. Venyaminov, Eur. J. Biochem. 119 (1981) 619–624.
[38] Y.V. Matsuka, L.V. Medved, S.A. Brew, K.C. Ingham, J. Biol. Chem. 269 (1994) 9539–9546.
[39] C. Tanford, Protein denaturation, in: C.B. Anfinsen, M.L. Anson, J.T. Edsall, F.M. Richards (Eds.), Adv. Protein Chem., Academic Press, New York, 1968, p. 23.
[40] W.K. Surewicz, J.J. Leddy, H.H. Mantsch, Biochemistry 29 (1990) 8106–8111.
[41] U. Dornberger, D. Fandrei, J. Backmann, W. Hubner, K. Rahmelow, K.-H. Guhrs, M. Hartmann, B. Schlott, H. Fritzsche, Biochim. Biophys. Acta 1294 (1996) 168–176.
[42] A. Muga, J.L.R. Arrondo, T. Bellon, J. Sancho, C. Bernabeu, Arch. Biochem. Biophys. 300 (1993) 451–457.
[43] B.K. Mohney, E.T. Petri, V. Uvarova, G.C. Walker, Appl. Spectrosc. 54 (2000) 9–14.
[44] Y. Fang, D.G. Dalgleish, J. Colloid Interface Sci. 196 (1997) 292–298.
[45] D. Reinstadler, H. Fabian, J. Backmann, D. Naumann, Biochemistry 35 (1996) 15822–15830.
[46] M. Jackson, P.I. Haris, D. Chapman, Biochemistry 30 (1991) 9681–9686.
[47] A.-F. Allain, P. Paquin, M. Subirade, Int. J. Biol. Macromol. 26 (1999) 337–344.
[48] T. Nagano, Y. Mori, K. Nishinari, Biopolymers 34 (1994) 293–298.
[49] H. Fabian, C. Schultz, D. Naumann, O. Landt, U. Hahn, W. Saenger, J. Mol. Biol. 232 (1993) 967–981.